Sixth International Symposium on Turbulence and Shear Flow Phenomena
Seoul, Korea, 22-24 June 2009

INFLUENCES OF BACKGROUND NOISE ON AUTO-GENERATION OF NEAR-WALL VORTICAL STRUCTURES IN A CHANNEL FLOW

Kyoungyoun Kim
Department of Mechanical Engineering,
Hanbat National University
San 16-1, Duckmyoung-dong, Yuseong-gu, Daejeon 305-719, Korea
kkim@hanbat.ac.kr

Hyung Jin Sung
Department of Mechanical Engineering,
KAIST
373-1 Guseong-dong, Yuseong-gu, Daejeon 305-701, Korea
hjsung@kaist.ac.kr

Ronald J. Adrian
Department of Mechanical and Aerospace Engineering
Arizona State University
Tempe, Arizona 85287, USA
rjadrian@asu.edu

ABSTRACT

We examine the auto-generation process by which new hairpin vortices are created from a sufficiently strong hairpin vortex, leading to the formation of a hairpin packet. The initial conditions are given by conditionally averaged flow fields associated with the second quadrant (Q2) event in the fully turbulent channel flow DNS database at Re_τ=395. The nonlinear evolution of the initial vortical structure is tracked by performing a spectral simulation. Background noise is introduced by adding small amplitude perturbations to the initial field or by imposing momentum forcing. The background noise gives rise to chaotic development of a hairpin packet. The hairpins become asymmetric, leading to much more complicated packet structures than are observed in the symmetric hairpin vortex train of the flow with a clean background. However, the chaotic packets show the same properties as the clean packet in terms of the rate of growth of vertical and spanwise dimensions and the distance between successive vortices, suggesting that the auto-generation mechanism is robust. The background noise leads to a decrease in the minimum value of the Q2 strength required to trigger auto-generation, indicating that background noise enhances auto-generation, especially in the buffer layer. The auto-generation process is more enhanced by the background noise with wavenumbers $k_x < k_z$. Finally, the auto-generation process was tested in a real turbulent environment taken from an instantaneous field of a turbulent channel flow DNS.

INTRODUCTION

Coherent structures in wall turbulence are of great importance since they transport momentum and provide a means of producing turbulent kinetic energy (Adrian, 2007). The organization of hairpin vortices into packets and the interactions between these packets are characteristic features of wall turbulence that explain many experimental measurements and observations, including the inordinately large amount of streamwise kinetic energy residing in very long streamwise wavelengths (Kim and Adrian, 1999), the occurrence of multiple second quadrant (Q2) events in turbulent bursts (Luchik and Tiederman, 1987; Tardu, 1995), the formation of new streamwise vortices, and characteristic angles of inclined hairpins (Adrian et al., 2000). Further, hairpin vortex packets play an important role in the production of the Reynolds shear stress, which is directly related to the turbulent drag. Ganapathisubramani *et al.* (2003) showed that the vortex packet contributes significantly (about 25%) to the total production of Reynolds shear stress in the log-layer of turbulent boundary layers. In addition to the experimental observation of hairpin packets in instantaneous flow fields using PIV, statistical evidence of hairpin packets has been reported by Christensen and Adrian (2001) and Hambleton *et al.* (2006). Specifically, using linear stochastic estimation (LSE) of the conditionally averaged flow field associated with a swirling motion, they found a series of swirling motions located along a line inclined at 12-13^o with respect to the wall. Zhou *et al.* (1999) proposed an auto-generation mechanism for hairpin formation, whereby new hairpins are successively generated from a parent vortex and formed into a packet. Subsequently, in a dynamical simulation study of a low Reynolds number channel flow (Re_τ=180), Zhou *et al.* (1999) examined the evolution of the initial vortex extracted

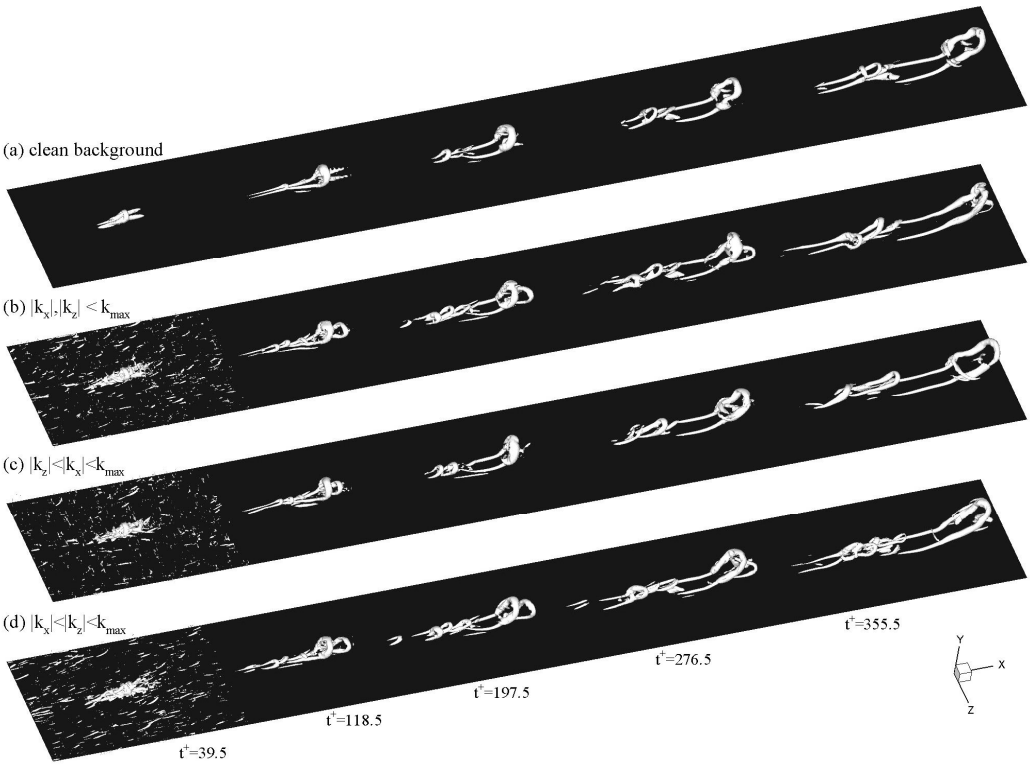

Fig. 1 Time-evolution of initial vortical structure extracted by Q2 event vector of strength α=3 specified at y_m^+=51.3. The three-dimensional structures represent iso-surfaces of the vortex swirling strength, $\lambda_{ci}h/u_\tau$=15. The background noises are uniformly distributed over the specified wavenumber domain and the magnitudes are selected so that their r.m.s. values in the physical domain are 40% of the fully turbulent DNS results.

by the conditionally averaged field associated with the Q2 event in the channel flow. They found that an initial vortex whose strength exceeds a certain threshold value can auto-generate a secondary hairpin, which in turn generates a tertiary hairpin, and so on. These hairpin vortices organize themselves such that they move downstream in a group with little dispersion, giving rise to a packet of hairpin vortices. Zhou *et al.* (1999) also showed that asymmetric initial vortices grow more rapidly than symmetric ones, and hence are likely to be the most common form found in natural wall turbulence. Adrian and Liu (2002) explored the effect of initial asymmetry on the evolution of the initial eddy by performing a dynamical simulation at a higher Reynolds number (Re_τ=300). The initial field has a small asymmetry, 5% with respect to reflections about the streamwise plane of the vortex center. As such initial vortices with small asymmetry evolve, a highly complicated packet is developed. This packet contains many hairpins that have the form of a cane or a one-legged hairpin, and appears as a complicated and apparently chaotic entity due to the considerable amount of interactions associated with self-induction. The chaotic packets observed in the dynamical simulations have many similarities to the hairpin packets observed in fully turbulent simulations (Liu and Adrian, 1999). However, in the former study, the effects of asymmetry (or perturbation) in the initial condition on the chaotic packet formation were not examined in a systematic way because the initial perturbation was introduced from a sampling error in forming the correlation tensor needed to extract the initial vortex.

In the present study, the effects of background noise on the auto-generation and formation of chaotic hairpin packets are investigated by performing a series of dynamical simulations. Similarly to Zhou *et al.* (1999), the initial vortices were extracted by LSE of the conditionally averaged field associated with the Reynolds shear stress producing the Q2 event in fully turbulent channel DNS data at Re_τ=395. The results show that the auto-generation process is robust to the presence of background noise in terms of global properties, however, it is more enhanced by the background noise with wavenumbers $k_x<k_z$. Finally, the auto-generation mechanism is tested in real turbulent flow fields.

NUMERICAL METHODS

In the present study, the evolution of an initially isolated vortical structure is tracked by performing a dynamical simulation of the channel flow with constant mean pressure gradient. The non-dimensional governing equations of an unsteady, incompressible flow are

$$\nabla \cdot \mathbf{u} = 0 \tag{1}$$

$$\frac{\partial \mathbf{u}}{\partial t} + \mathbf{u} \cdot \nabla \mathbf{u} = -\nabla p + \frac{1}{\mathrm{Re}_\tau} \nabla^2 \mathbf{u} \tag{2}$$

, where $\boldsymbol{u}$ is the velocity and p is the pressure. The streamwise, wall-normal and spanwise coordinates and velocity components are, respectively, x, y, z and u, v, w. The friction velocity u_τ and the channel half-height h are used as the velocity and length scales, respectively. The Reynolds number is defined as $Re_\tau = u_\tau h/\nu$, where ν is the kinematic viscosity.

Time-integration of the governing equations is achieved by a semi-implicit method. For spatial derivatives, a spectral method is used with Fourier representations in the streamwise and spanwise directions, and Chebyshev expansion in the wall-normal direction. Periodic boundary conditions are applied in the streamwise and spanwise directions, and the no-slip boundary condition is imposed on the velocities at the solid walls. The domain size is $2\pi h \times 2h \times \pi h$ in the streamwise, wall-normal and spanwise directions, respectively. After testing several grid resolutions, 128×128×192 spectral modes were used, which corresponds to Δx^+=19.4, Δy^+=0.12~9.69 and Δz^+=6.46.

The initially isolated vortices are extracted from the conditionally averaged flow fields associated with Reynolds stress producing events from the DNS data of fully developed turbulent channel flow at Re_τ=395:

$$\mathbf{u}(\mathbf{x}, t=0) = \overline{\mathbf{u}}(y) + \left\langle \mathbf{u}'(\mathbf{x}) \mid \mathbf{u}'(y_m) = \alpha(u_m, v_m, 0) \right\rangle \quad (3)$$

, where the overbar denotes a time average. The events (u_m, v_m) are found from the maximum value of the probability weighted Reynolds shear stress $u'v'$ pdf(u',v') (Moin et al., 1987). The amplification factor (α) is referred to here as the strength of the Q2 event. Since a true conditional average is statistically very hard to obtain, especially as the condition becomes complicated, we approximate the conditional average with a linear stochastic estimation (Adrian, 1996) in the present study.

RESULTS AND DISCUSSION

Auto-generation of hairpin vortices in the presence of initial background noise

To examine the effect of background noise on the formation of new hairpin vortices, we tested the auto-generation mechanism in the presence of initial background noise ($\boldsymbol{u}_{\text{noise}}$). The Fourier coefficients of the background noise,

$$F\{\mathbf{u}_{noise}\}(k_x, y, k_z) = \left|F\{\mathbf{u}_{noise}\}\right|(k_x, y, k_z)e^{i\phi} \quad (4)$$

have constant magnitude over the wavernumber domain (k_x, k_z) and random phases. The coefficient magnitudes are scaled such that r.m.s values of $\boldsymbol{u}_{\text{noise}}$ are 40% of those of fluctuating velocities in the fully turbulent DNS data and the random phase of the noise (ϕ) is imposed with uniform probability density over 0 to 2π. We tested three distinct types of background noise, which are specified over the wavenumber domain: $|k_x|$ & $|k_z| < k_{max}$, $|k_z|<|k_x|<k_{max}$ and $|k_x|<|k_z|<k_{max}$. Here, k_{max} is the maximum wavenumber which

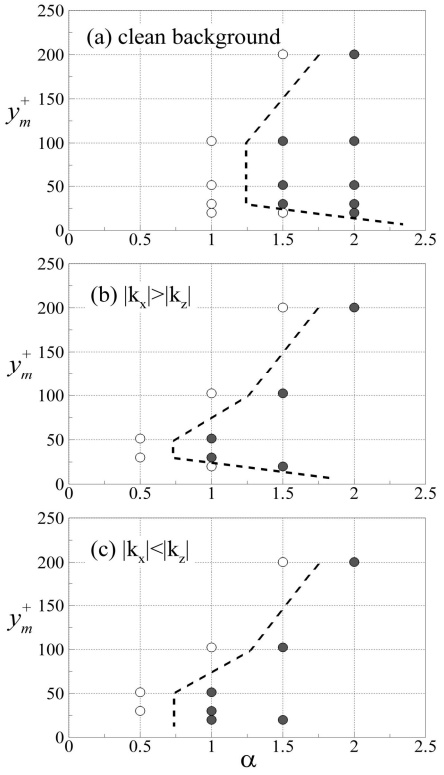

Fig. 2 The generation of secondary hairpin vortices depends on the strength of initial vortical structures and location of the event vector used to extract the initial vortical structure. ●: case with new hairpins, ○: case without new hairpin. (a) clean background (b) background noise distributed over $|k_x|>|k_z|$ and (c) background noise distributed over $|k_x|<|k_z|$.

can be resolved in the present simulation. In each case, the background noise is superimposed onto the initial flow field obtained by LSE with the Q2 event in Eq. (3). Figure 1 shows the evolutions of initial vortical structures in the presence of the different types of background noise. Due to the initial background noise, the vortices have an asymmetric shape in the spanwise direction. New vortex generation behavior, in particular the shape and number of newly generated vortices, differs among the systems with different background noise types. In addition, the flows with background noise show chaotic behavior; however, the chaotic packets retain the same general properties as the clean packet in terms of distance between the primary and secondary hairpin vortices (PHV and SHV), and vertical and spanwise growth rate. This robustness is consistent with turbulence being random, yet having reproducible statistical properties (Adrian, 2007).

The global properties of the auto-generation are almost the same for all systems, regardless of the presence and type of background noise; however, the details of auto-generation are sensitive to the initial background noise. It is reported that the generation of secondary hairpin vortices is possible only if the initial structures are sufficiently strong (Zhou *et al.*, 1999). To examine the effect of initial

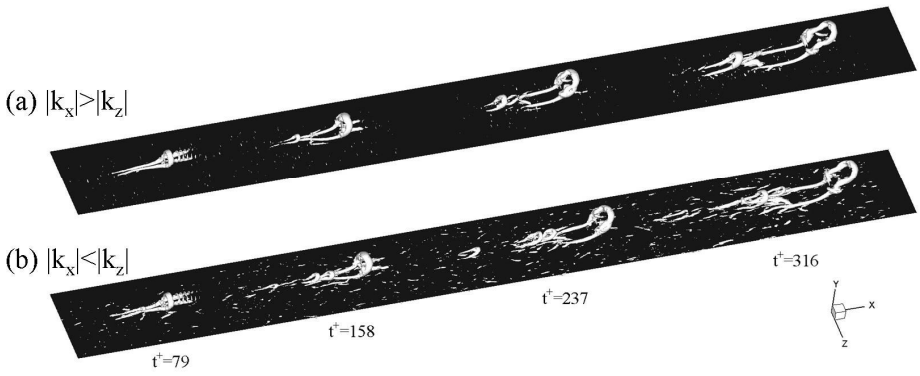

Fig. 3 Time-evolution of initial vortical structure extracted by the Q2 event vector of strength α=3 specified at y_m^+=51.3. The three-dimensional structures represent iso-surfaces of the vortex swirling strength, $\lambda_{ci}h/u_\tau$=15. The background noises are uniformly distributed over the specified wavenumber domain and sustained in time through the Ornstein –Uhlenbeck process.

background noise on the threshold for auto-generation, we performed a series of dynamical simulations with many different initial vortices in the presence of initial background noise, as well as with a clean background. The generation of secondary hairpin vortices depends on the strength α and location y_m^+ of the Q2 event vector used to extract the initial vortical structures. In the case of a clean background (Fig. 2a), an optimum distance of the initial vortex from the wall for auto-generation is observed in the buffer layer, consistent with previous results (Zhou *et al.*, 1999) from simulations of flows with the lower Reynolds number of Re_τ= 180. The existence of this optimal location was explained in terms of a balance between the lifting-up and backward curling of vortices due to vortex-induced motion of QSV legs and vortex stretching due to the mean shear. In the presence of background noise (Figs. 2b and 2c), the threshold behaviors for the auto-generation show similar patterns to the results without initial background noise. However, the minimum Q2 event strength required to trigger the generation of secondary vortices becomes lower due to the background noise. A closer comparison between Figs. 2b and 2c reveals that the perturbations with $|k_x|<|k_z|$ further decrease the threshold value for the auto-generation from the initial vortex associated with the Q2 event at y_m^+=20. These findings suggest that the presence of background noise enhances the auto-generation of secondary hairpin vortices, especially in the buffer layer, and the perturbations with $|k_x|<|k_z|$ are more effective to the enhancement than those with $|k_x|>|k_z|$.

Auto-generation of hairpin vortices in the presence of a sustained background noise

Since the white-noise perturbations on the initial vortical structure decay in a relatively short time, the interaction between the auto-generation process and the background noise could be less as time goes by. To see the effect of background noise on the auto-generation process including the evolution of a '*mature*' hairpin packet, it is required to test the auto-generation process in the presence of a sustained random noise. In order to examine the auto-generation process with a sustained background noise, we perform additional simulations by including a random forcing term in the momentum equations. The random forcing $F_i(x,y,z,t)$ is obtained from the Ornstein -Uhlenbeck (O-U) random process (Pope, 2000) as follows:

$$d\hat{F}_i(k_x,y,k_z,t) = -\frac{\hat{F}_i}{\tau}dt + \left(\frac{2\sigma^2}{\tau}\right)^{1/2} dW \qquad (5)$$

where $\hat{F}_i(k_x,y,k_z,t)$ is the Fourier coefficient of the random forcing and dW is the Wiener process. The O-U process is a statistically stationary normal process with the integral time scale of τ and variance of σ. In the present study, the integral time scale is chosen as 4 $[(\nu/u_\tau^2)(h/U_{y=h})]^{1/2}$, which was reported as the most probable duration of acceleration events in turbulent channel flows (Alfredsson and Johansson, 1984). The Fourier mode of the random forcing is nonzero for the wavenumber domain $|k_x|<|k_z|<k_{max}$ or $|k_z|<|k_x|<k_{max}$. The variance σ is scaled such that the r.m.s. values of $F_i(x,y,z,t)$ are 15% of $(\partial p'/\partial x_i)_{rms}$ in the fully turbulent DNS data, which is dependent on the wall distance and thus it could reflect the inhomogeneous interaction between the hairpin vortices and their background turbulence.

Figure 3 shows the evolution of initial vortical structures in the presence of the above random forcing. The initial vortical structure is extracted by the Q2 event of α=3 specified at y_m^+ =51.3. As expected, the background noise is observed at every time step due to the random forcing. Although the random forcing makes a different environment of the vortex evolution, i.e., sustained background noise, the auto-generation process shows nearly the same behavior as that under temporally decaying perturbations. The hairpin vortices make a packet which has nearly the same convection velocity and most of new vortices are generated at upstream of the parent vortices. This suggests that the evolution of the '*mature*' packet is also robust to the background noise as well as the evolution of single hairpin (Fig. 1). Regarding the effect of spectral domain of the imposed random forcing, the generation of new vortices is

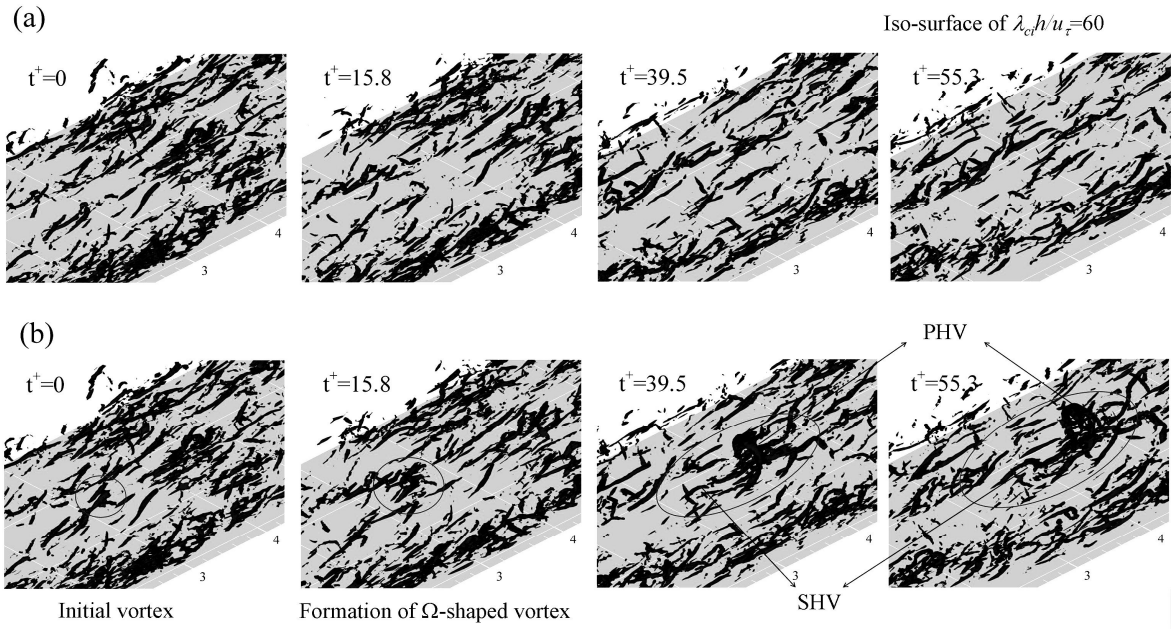

Fig. 4 (a) Snapshots of near-wall vortical structures taken from DNS of turbulent channel flow (Re_τ=395). (b) Evolution of hairpin vortex superimposed to the turbulent flow field of t^+=0 in (a). The initial hairpin vortex is extracted by LSE with α=6 and y_m^+=50.

more enhanced by the random forcing with $|k_x|<|k_z|$ (Fig. 3b) as compared with $|k_x|>|k_z|$ (Fig. 3a). This is consistent with the observation in the evolution of the initially perturbed flow structure as shown in Fig. 1. We also tested a distinct initial vortical structure at y_m^+=30.1 and the same conclusion could be drawn.

Auto-generation of hairpin vortices in fully turbulent channel flows

Finally, we examine the auto-generation mechanism in real turbulent flow fields. An initially isolated vortex obtained by LSE with α=6 and y_m^+=51.3 was evolved in a turbulent fluctuating velocity field taken from an instantaneous flow field of a DNS database. For comparison, snapshots of near-wall vortical structures in a DNS of turbulent channel flow are shown in Fig. 4a. The evolution of the initial vortex (Fig. 4b) can be clearly seen by comparing the DNS field at the same evolution time. At t^+=0, the initial vortex comprises a pair of quasi-streamwise vortices and is slightly distorted due to the strong turbulent fluctuating fields. The size and strength of the initial vortical structure are comparable to those of the near-wall vortical structures in the real turbulent flow field. At t^+=15.8, an Ω-shaped vortex is formed from the initial vortex, and this Ω-shaped vortex then develops into the primary hairpin vortex. At t^+=39.5, the SHV starts to be generated upstream of the PHV, and it becomes cane-like vortices later. A cane-like SHV was previously observed in the auto-generation mechanism starting from an asymmetric initial vortex (Zhou *et al.*, 1999). Although we imposed a symmetric initial vortex, a cane-like highly asymmetric vortex is generated, consistent with previous observations that asymmetric hairpins with a single leg are more common in fully turbulent flows (Robinson, 1991). The overall process of auto-generation in the fully turbulent flows is very similar to that described in the previous section. Figure 4 clearly shows that auto-generation can occur in real turbulent flows if the initial vortex is sufficiently strong. We also tested a weaker initial vortex with α=3; in that system, the vortex strength was so small that the initial vortex and its evolution were invisible.

CONCLUSIONS

We have examined the nonlinear evolution of an initially isolated vortex in the presence of background noise by performing a series of spectral simulations of channel flow. The initially isolated vortex was extracted by LSE of conditional flow fields associated with the Q2 event in the fully turbulent channel flow DNS database at Re_τ= 395. Background white noise corresponding to 40% of the r.m.s. of turbulent fluctuating velocities was superimposed onto the initial field, with three types of noise being considered. The initial background noise leads to chaotic development of the hairpin packet. The hairpins become asymmetric, giving rise to much more complicated packet structures than are observed for the symmetric hairpin vortex train of the clean background. However, the chaotic packets showed the same properties as the clean packet in terms of the rate of growth of the vertical and spanwise dimensions and the distance between successive vortices, suggesting that the auto-generation mechanism is robust. However, the details of auto-generation were found to be sensitive to the initial background noise. Initial random noise with $k_x<k_z$ enhanced secondary vortex generation to a greater degree than noise

with $k_x>k_z$, even though both initial noise types had the same amplitudes. A series of dynamical simulations of many different initial vortices revealed that the background noise decreases the minimum Q2 strength required to trigger auto-generation. Thus, background noise enhances auto-generation, especially in the buffer layer. The auto-generation process with a sustained background noise imposed by momentum forcing has shown to be similar to that with the initial background noise. The auto-generation process is more enhanced by the background noise with wavenumbers $k_x<k_z$ as compared with $k_x>k_z$. Finally, the auto-generation mechanism was examined in a real turbulent environment taken from the instantaneous field of a turbulent channel flow DNS. The generation of a secondary hairpin vortex was clearly observed upstream of the primary hairpin in a manner very similar to the cases with the clean background and artificial noise.

REFERENCES

Adrian, R. J., 1996, Stochastic estimation of the structure of turbulent flows. Eddy Structure Identification. J. P. Bonnet, Springer**:** 145-196.

Adrian, R. J., 2007, "Hairpin vortex organization in wall turbulence," *Physics of Fluids*, Vol. 19, pp. 041301.

Adrian, R. J. and Liu, Z. C., 2002, "Observation of vortex packets in direct numerical simulation of fully turbulent channel flow," *Journal of Visualization*, Vol. 5, pp. 9-19.

Adrian, R. J., Meinhart, C. D. and Tomkins, C. D., 2000, "Vortex organization in the outer region of the turbulent boundary layer," *Journal of Fluid Mechanics*, Vol. 422, pp. 1-54.

Alfredsson, P. H. and Johansson, A. V., 1984, "Time scales in turbulent channel flow," *Physics of Fluids*, Vol. 27, pp. 1974.

Christensen, K. T. and Adrian, R. J., 2001, "Statistical evidence of hairpin vortex packets in wall turbulence," *Journal of Fluid Mechanics*, Vol. 431, pp. 433-443.

Ganapathisubramani, B., Longmire, E. K. and Marusic, I., 2003, "Characteristics of vortex packets in turbulent boundary layers," *Journal of Fluid Mechanics*, Vol. 478, pp. 35-46.

Hambleton, W. T., Hutchins, N. and Marusic, I., 2006, "Simultaneous orthogonal-plane particle image velocimetry measurements in a turbulent boundary layer," *Journal of Fluid Mechanics*, Vol. 560, pp. 53-64.

Kim, K. C. and Adrian, R. J., 1999, "Very large-scale motion in the outer layer," *Physics of Fluids*, Vol. 11, pp. 417-422.

Liu, Z.-C. and Adrian, R. J., 1999, "Evidence for hairpin packet structure in DNS channel flow," *Turbulence and Shear Flow-1, First International Symposium*, Wallingford, U.K.

Luchik, T. S. and Tiederman, W. G., 1987, "Characteristics of ejections in turbulent channel flow," *Journal of Fluid Mechanics*, Vol. 174, pp. 529-552.

Moin, P., Adrian, R. J. and Kim, J., 1987, "Stochastic estimation of organized structures in turbulent channel flow," *Proc. 6th Turbulent Shear Flow Symp.*, Toulouse.

Pope, S. B., 2000, Turbulent Flows, Cambridge University Press.

Robinson, S. K., 1991, "Coherent motions in the turbulent boundary layer," *Annual Review of Fluid Mechanics*, Vol. 23, pp. 601-639.

Tardu, S., 1995, "Characteristics of single and clusters of bursting events in the inner layer, Part 1: Vita events," *Experiments in Fluids*, Vol. 20, pp. 112-124.

Zhou, J., Adrian, R. J., Balachandar, S. and Kendall, T. M., 1999, "Mechanisms for generating coherent packets of hairpin vortices in channel flow," *Journal of Fluid Mechanics*, Vol. 387, pp. 353-396.